



Estimation of Surface Temperature and Rainfall in Ghana

V.C.K. Kakane & H. Søggaard

Abstract

Daily Meteosat images for 1989 have been analysed for the purpose of mapping surface temperature and rainfall in Ghana. The images in the time-series are georeferenced and the maximum value composite (MVC) technique is applied to the temperature calibrated IR-channel images after a cloud screening of the images. The cloud covered areas are outlined and traced using the Meteosat visible channels. Stratiform clouds are detected using surface albedo while cumuliiform clouds are detected based on a technique calculating the spatial variability within a 5 pixel by 5 pixel window around each point in the image. The cloud covered parts of the scene are then delimited by comparing the normal albedo values and the spatial variance in albedo.

The paper then discusses how the outlined procedure can be applied in an environmental monitoring context. For each of the months June to November 1989 the mean monthly rainfall amounts

at 35 meteorological stations are plotted against the mean surface temperature. It is found that apart from the month of June statistical significant linear relationships are obtained and that the scattering around the line is decreasing for increasing sampling length.

Key Words

Meteosat AIVH data, NOAA AVHRR, visible image, albedo, infra red image, surface temperature, delimiting cloud, albedo variance, rainfall correlation.

V.C.K. Kakane, Physics Department, University of Ghana, Legon, Ghana.

H. Søggaard, University of Copenhagen, Institute of Geography, Øster Volgade 10, Copenhagen, Denmark.

Geografisk Tidsskrift, Danish Journal of Geography 97: 76-85, 1997.

In recent years substantial efforts have been applied to develop satellite-based techniques for monitoring environmental surface conditions. One of these has been the use of surface temperatures measured by satellites to estimate rainfall and evapotranspiration. These studies have mostly been concentrated in the Sahelian Regions (latitude 10° - 20°) of the West African region. The potential use of Meteosat thermal infrared data has been comprehensively documented (Rosema, 1982). Since then a number of studies (Seguin et al, 1989; Imbernon et al, 1990) have analysed these data for environmental monitoring purposes and by Milford and Dugdale, 1990, for rainfall monitoring using the so-called cold cloud duration technique. One particular use is that of ground surface temperatures to estimate evapotranspiration. In this regard, the combination of NOAA-AVHRR satellite data and a agrometeorological model was demonstrated by Lagouarde, 1991.

In the present approach it is utilised that rainfall on a hot land surface will cause a drop in surface temperature as a

large fraction of the incoming radiation will be used for evaporation rather than heating of soil and atmosphere. After the passage of a tropical squall line system the drop in surface temperature due to increased evaporation rate can have a magnitude of 8-10 °C (Søggaard, 1989). The use of ground surface temperatures to quantitatively estimate rainfall has already been studied by Kakane & Imbernon, 1992, using NOAA-AVHRR data.

Conceptually this application can be examined by use of the surface energy balance. On a daily basis it can be assumed that the net radiation flux (R_n) at the surface is balanced by the energy used for evaporation (Q_e) and heating of the atmosphere (Q_h):

$$R_n = Q_h + Q_e \quad [1]$$

The unit for all three terms is MJ m⁻² d⁻¹. As demonstrated for the shahelian environment (Søggaard, 1988) the sensible heat flux can be expressed as linear function of the

surface temperature:

$$Q_n = c_1 \cdot T_s + c_2 \quad [2]$$

where

c_1 and c_2 are environment/climate specific "constants" in ($\text{MJ m}^{-2} \text{d}^{-1} \text{K}^{-1}$) and ($\text{MJ m}^{-2} \text{d}^{-1}$) respectively, T_s is the surface temperature ($^{\circ}\text{C}$).

The net radiation can be estimated either from satellite images or ground observations while the surface temperature can be obtained from the infrared satellite data, and consequently equation [1] and [2] can then be solved for the energy used for evaporation ($\text{MJ m}^{-2} \text{d}^{-1}$). This can be converted to mm of evapotranspiration per day simply by dividing by the latent heat of vaporization ($\lambda=2.47 \text{ MJ kg}^{-1}$).

For practical purposes it is, however, very difficult to calibrate the method as the field observations of Q_e are very sparse in general and also in Ghana. Instead it is here proposed to run the method against rainfall utilizing the fact that in warm climates with relatively low rainfall rates (i.e. less than the potential evapotranspiration), as found in most places in Ghana, it can be assumed that the monthly mean rainfall (P) and the evapotranspiration are highly correlated. It is also assumed that the net radiation on a mean daily basis is relatively constant. Consequently, equation [1] and [2] can be rearranged to the following:

$$P = a + b \cdot T_s \quad [3]$$

where the constants

$$a = (R_n - c_2) / \lambda \quad (\text{mm d}^{-1})$$

$$b = -c_1 / \lambda \quad (\text{mm d}^{-1} \text{K}^{-1})$$

and P is the monthly rainfall converted to daily mean (mm d^{-1})

In this method, pluviometry is not linked to a rainfall occurrence probability, but to its signature on the ground, through the effect that a previous rain has had on the ground temperature. For practical applications it is however found that extensive cloud cover, particularly during the rainy season, often limits the number of nearly "cloud-free" scenes.

One way of overcoming this problem is to use the maximum value composite (MVC) technique (Holben, 1986). This technique reduces the influence of clouds and mini-

mizes atmospheric absorption effects due to water vapour. This paper discusses the possible application of this method to Ghana (latitude 5°N - 10°N) for environmental monitoring and investigates if the technique can be applied under to equatorial conditions.

Location, Methods and Materials.

The study area consists of the southern part of Ghana as shown in Figure 1. Due to the differences in rain patterns between the northern and southern parts of the country, it is decided to limit the present study to the south. This area lies at the Guinea Coast and even though it is normally assumed to be climatically characterized by a uniform rainfall distribution throughout the year (Nicholson, 1994), spatial as well as temporal variations in rainfall are found (Dickson & Benneh, 1995). Maximum values occur in June/July. The region is more humid than the north and has two rainy seasons separated by a dry period, normally around August. The yearly rainfall amount is highest in the south-western part of the country, and decreases as one goes eastwards along the coast, which is the driest part of the country. Rainfall also increases with elevation. Annual rainfall values per station are in the range between 700 mm and 2500 mm. Figure 1 shows mean monthly rainfall for two stations, one in the middle and the other at the coast. The mean monthly temperature is around 27°C - 30°C throughout the year.

Ground reference data

Decadal (10-day) ground rainfall measurements were provided for the southern part shown in Figure 1 by the Ghana Meteorological Services Department. About 50 rainfall stations are found. After eliminating stations with incomplete data, 35 stations were left for the final analysis.

Satellite data

All the Meteosat data used in the present study have been provided by the Danish Meteorological Institute. One situation has been selected for each day during the 5-month period. To ease comparison with NOAA-AVHRR data, the METEOSAT (AIVH) data were selected to coincide, as much as possible, with the local time of the NOAA-11 afternoon overpass (14-15h local time).

The Meteosat data have been processed at the Institute of Geography using the CHIPS software (1992). From each

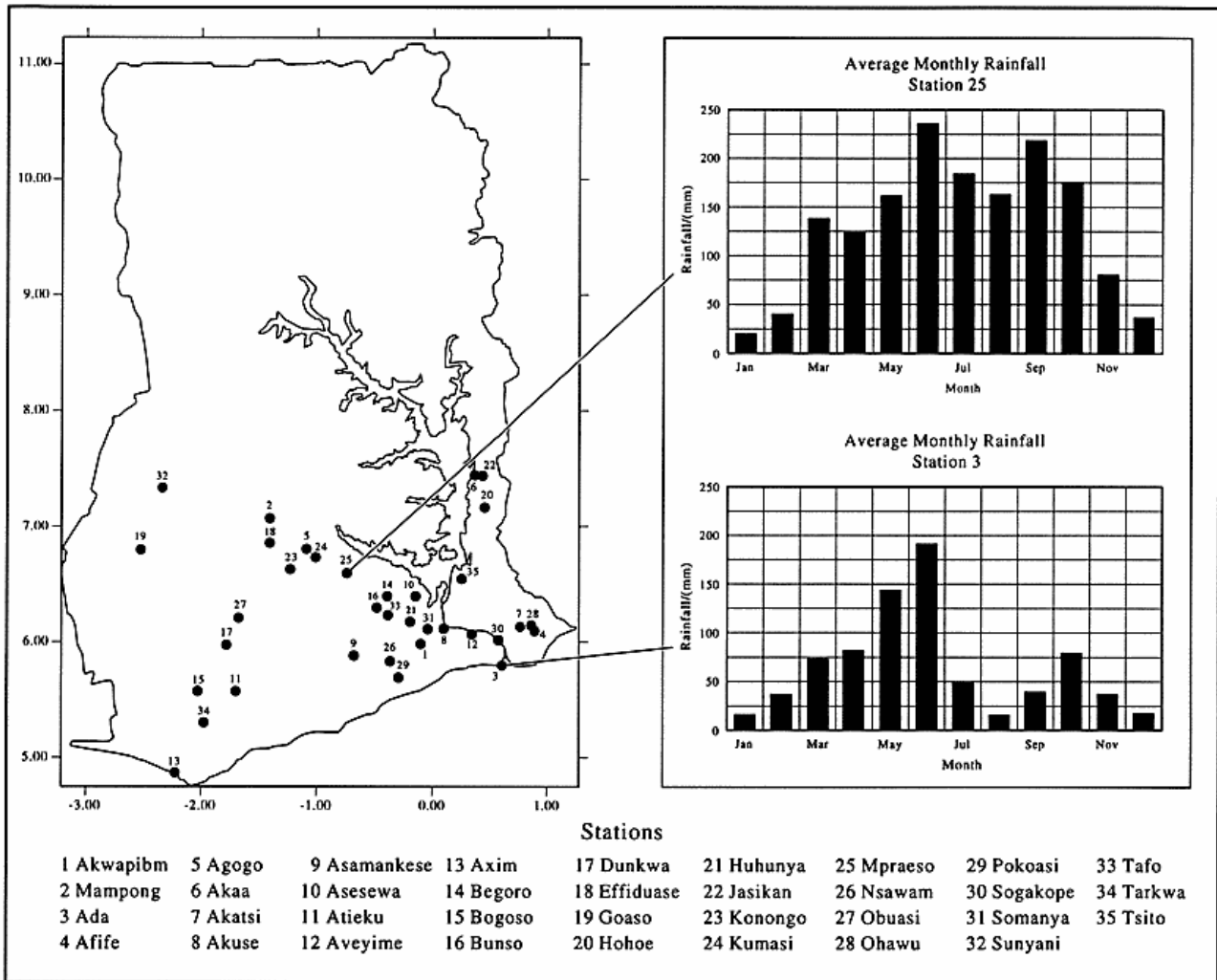


Figure 1: Map showing stations used.

case a 512x512 pixel region covering Western Africa was selected.

The cases were geometrically corrected using a second-order polynomial to the UTM-coordinate system. The visible data were transformed to albedo using the expression, presented in Sogaard, 1990

$$\text{albedo}(i,j) = c_{\text{vis}} \frac{[\text{VIS}_{\text{DN}}(i,j) - \text{VIS}_{\text{DN}}(\text{space})]}{(\cos z)^{1.2}} \quad (1)$$

where

z is the solar zenith angle,

$c_{\text{vis}} = 0.45$ (an empirically-estimated coefficient),

$\text{VIS}_{\text{DN}}(i,j)$ is the digital number (0 - 255) in the visible channel recorded by satellite when viewing pixel (i,j) , and $\text{VIS}_{\text{DN}}(\text{space})$ is the digital number (0 - 255) in the visible channel recorded by satellite when viewing space.

Figure 2 shows the temporal albedo variation from beginning of June to end of November. During this period the albedo decreases from 0.25 to around 0.15. This general trend is, however, different where the actual pixel is contaminated due to dense cloud cover, increasing albedo values to between 0.8 and 0.9. To overcome this problem an analysis procedure has been elaborated for producing non-contaminated albedo images.

The IR-data have been recalculated to radiance and

further on to brightness temperature using the following expression

$$T_s(i,j) = B^{-1} c_{ir} [IR_{DN}(i,j) - IR_{DN}(space)] \quad (2)$$

where

T_s is the surface temperature, as measured from a satellite without atmospheric correction and assuming a surface emissivity of 1, (K),

B^{-1} is the Inverse Planck function (Stephens, 1994),

c_{ir} is the IR calibration coefficient as published in Meteosat Exploitation Project (1989),

$IR_{DN}(i,j)$ is the digital number (0 - 255) in an infrared channel recorded by the satellite when viewing pixel(i,j), and $IR_{DN}(space)$ is the digital number (0 - 255) in an infrared channel recorded by the satellite when viewing space.

In practice, for deriving B^{-1} , a weighted Planck function published as a look-up table (Meteosat Exploitation Project, 1989) was applied.

To correct for atmospheric attenuation due to water vapour, radiosonde data were analysed. This correction is based on a model using radiosonde data (Price, 1983) as input parameters. The model was slightly modified to take into account of the radiometer characteristics of Meteosat (Søgaard, 1990). Due to lack of data from Ghana the radio-

Table 1: Monthly Precipitable Water (Pw) and Temperature Correction (Tcorr).

Month	Pw, cm	Tcorr, °C
July	4.08	9.9
August	4.55	11.1
September	3.91	9.4
October	3.56	8.5

sonde data were collected from Niamey Airport, comprising daily observations measured at noon.

Besides the atmospheric water vapour content, the magnitude of the atmospheric correction also depends on the surface temperature. By comparison with field observation for the Niamey area, a mean temperature difference of 8°C was found between noon-time surface temperature and air temperature during this part of the season. This value was used in the model simulation of surface temperature at the radiosonde site. The time course of the correction showed maximum values in the middle of the rainfall season and decreasing values as the drying season proceeds. Due to the large spatial and temporal variation in atmospheric water vapour content, it was decided to estimate the correction on a monthly basis. Table 1 summarizes the mean monthly atmospheric temperature corrections used in the present study together with the mean precipitable water content in the atmosphere. Correction values used for June and November were those of July and October, respectively.

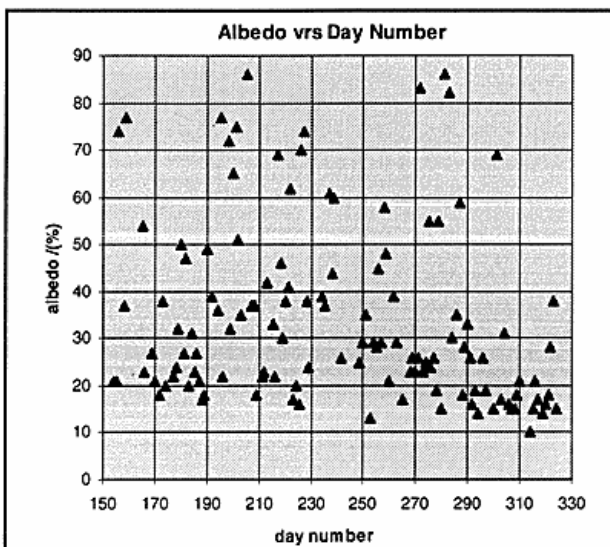


Figure 2: Variation of albedo with day number.

Delimitating clouds using visible images.

In theory the MVC-technique for obtaining surface temperature is straightforward. In certain cases, however, clouds may exist in each of the daily images in a ten-day interval and thus lead to erroneous conclusions. To tackle this problem a two-type cloud screening methodology technique was elaborated.

The first type is due to stratiform partly transparent clouds typically of the cirrus type. The stratiform clouds cause a general increase in albedo. The second type is due to cumuli clouds in which high albedo values are found on the sun exposed while the low values are found in the shadow of the cloud. To manage the cloud problem, a two-level classification scheme is described. Firstly, stratiform

clouds are detected by comparing the normalized albedo values for the actual period of the year. Secondly, cumuli clouds are detected by calculating the spatial variance within a 5 x 5 window around each pixel using equation 6.

$$\text{Pixvar}(i,j) = \frac{1}{25} \sum [X(i+m,j+n) - X_{\text{mean}}(i,j)]^2 \quad (3)$$

where

Pixvar(i,j) is the variance at pixel (i,j)

X(i,j) is the albedo value at pixel (i,j)

Xmean(i,j) is the mean albedo of the 25 pixel around pixel (i,j)

m = -2 .. 2

n = -2 .. 2

(See fx. Brisson *et. al.* (1990) and Gutman *et. al.* (1994).)

In areas with numerous small cumuli clouds, the albedo variance will increase from the background level of 1 or 2 digital counts to values in the region of 5 to 10 digital counts. Figure 3 shows a typical albedo image, with the corresponding variance and temperature images for the same day shown in Figures 4 and 5 respectively. The cloud-covered areas are delimited by rings of high variance values in Figure 4.

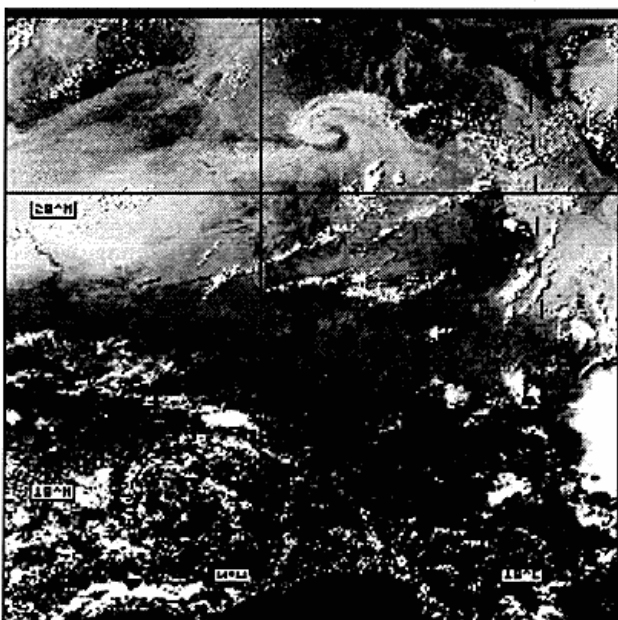


Figure 3: Albedo Image (02/07/89).

The effect of small cumuli clouds is demonstrated in Figure 6, which relates the albedo variance with surface temperature. The surface temperature is rather uniform around 20°C, whereas albedo variance is less than approximately 5 but from then on the clouds lead to



Figure 4: Albedo variance image (02/07/89).

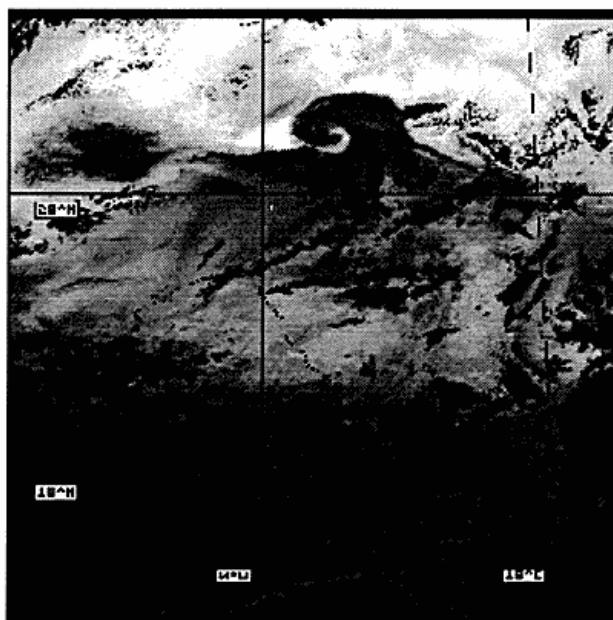


Figure 5: Temperature image (02/07/89). Dark areas show clouds.

increasing values of variance and decreasing temperature, as the pixels now become a mixture of cloud covered and cloud-free areas. If a pixel variance is greater than 5 then clouds are found and a temperature threshold of 0°C is assigned to that pixel. This condition is used to construct new temperature images (Figure 7). This threshold was chosen in order not to have negative temperature values and

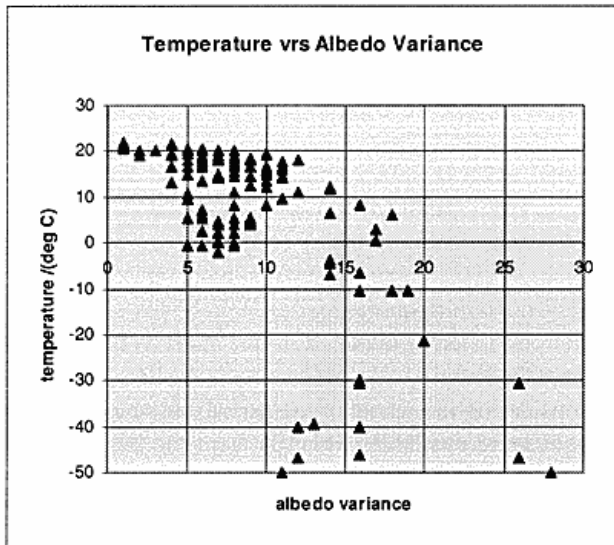


Figure 6: Variation of temperature with albedo variance.

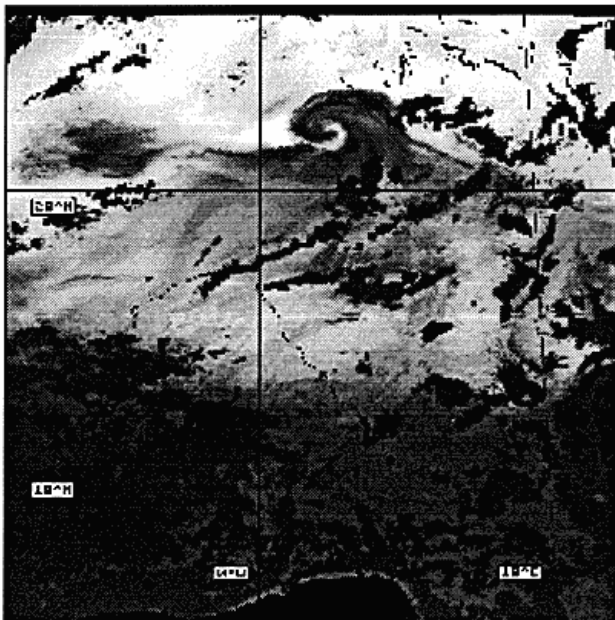


Figure 7: New temperature image; constructed (02/07/89).

not to augment the temperatures too much. A maximum value composite (MVC) technique was then performed using these new images on a 10 - day (decadal) basis (Figure 8). Some masked areas are still shown in this MVC image.

Correlation of temperature with rainfall

Temperatures were derived from the 10 - day MVC images for each of the stations. Correlation between rainfall (accumulated (ΣP) and mean (P_{mean})) and the mean surface temperature (T_{mean}) was carried out both on a monthly basis and for the total period (1st June to 20th November, 1989).

Table 2: $\Sigma P = a + b * T_{mean}$: Monthly analysis.

Month	a	b	r ²
June	320.6	-0.52	0.0003
July	545.6	-13.3	0.47
August	751.1	-20.7	0.54
September	454.3	-10.4	0.37
October	625.3	-18.0	0.58
November	346.7	-10.0	0.60

Table 3: $P_{mean} = a + b * T_{mean}$: Monthly analysis.

Month	a	b	r ²
June	10.7	-0.017	0.0003
July	17.6	-0.43	0.47
August	24.2	-0.67	0.54
September	15.1	-0.35	0.37
October	20.2	-0.60	0.58
November	17.3	-0.50	0.60

Table 4: $\Sigma P = a + b * \Sigma T$. Seasonal analysis.

Month	a	b	r ²
31st July	1139	-4.2	0.21
31st August	2190	-6.4	0.46
30th Sept.	2545	-4.6	0.36
31st October	3609	-6.8	0.57
20th	4123	-6.8	0.59

Beginning of data accumulation is on 1st June.



Figure 8: Maximum value composite temperature image (1st-10th July, 1989).

Results and discussion

The method of delimiting clouds shows encouraging results as the cloud-covered areas are seen as rings of high variance values.

The results of rain correlation with surface temperature are shown in Tables 2 to 4.

Typical regression lines are shown in Figures 9 (i-v). These figures show the evolution of rain during the period. July and August graphs show points scattered more

in the middle part. For September and October they are conglomerated more towards the upper part of the rainfall axes, while for November which is virtually the end of the rainfall period, the points are again uniformly distributed.

In Table 5, results of some previous work done in the Sahelian region are presented. These are results for relationships between cumulative rainfall (ΣP) and cumulative surface temperature (ΣT). The temperature values are the maximum value composites over a certain period. This period varies from seven to fifteen days. In such a case there will be no need for images during the whole period.

The correlation coefficients are lower than for the Sahel. The correlations have been found to improve in the Senegal when the air temperature is taken into account (Negre, 1987; Guillot, 1995). This was done by deducting the difference between the air temperature at each station and that of Dakar from the surface temperature. This was not considered in this study.

The coefficient a obtained in this study is higher than that for the Sahel.

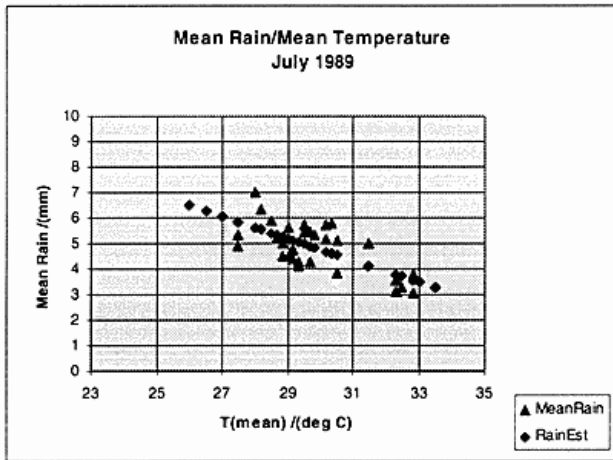
Considering the whole of the period for which satellite images were available, which is from the beginning of June to end of November, accumulated rainfall with mean temperature from Table 4 will give values of $a = 23.8$ and $b = -0.04$.

For the Senegal the corresponding values will be 18.1 and -0.04 obtained by Kakane & Imbernon (1992). Even though results for cumulative data are much higher in the present study than in Table 4, the mean values appear very close. It can also be seen in Table 5 that the values are not the same every year but show slight variations (Seguin et al., 1989).

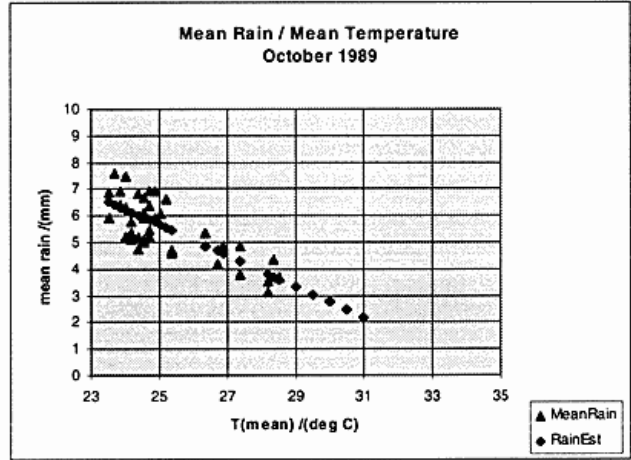
Table 5: Results of other studies.

Author	Year	Country	$\Sigma P = a + b \Sigma T$			$\Sigma P = a + b T_{mean}$			Satellite
			a	b	r^2	a	b	r^2	
Seguin et al. (1989)	1984	Senegal	1715	-2.88	0.93				Meteosat
	1985		1457	-2.52	0.84				
Negre (1987)	1984	Senegal				2146	-53.2	0.85	Meteosat
	1985					1912	-44.8	0.46	
	1986					2723	-64.5	0.72	
Kakane & Imbernon (1992)	1989	Senegal	2219	-5.4	0.80	2205	-42.5	0.79	NOAA-9

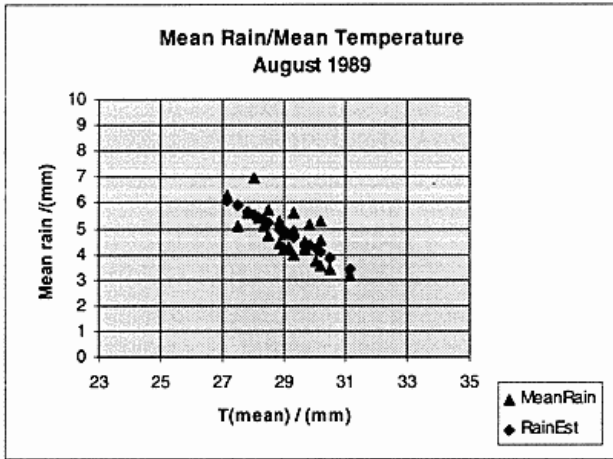
(i) July.



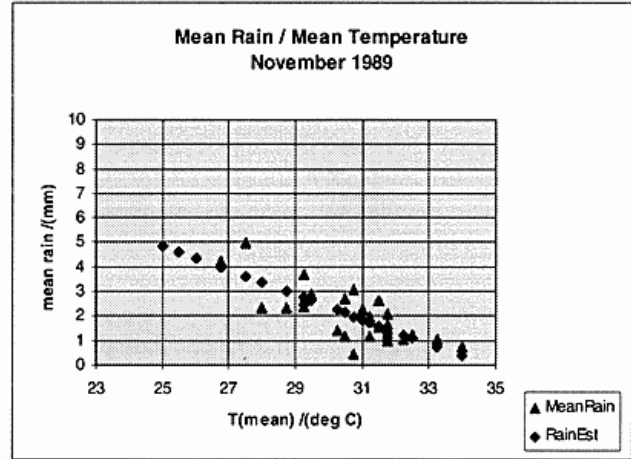
(iv) October



(ii) August



(v) November.



(iii) September.

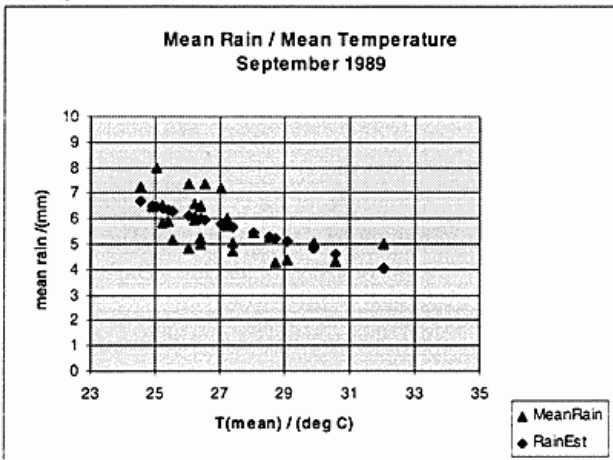


Figure 9: Monthly regression analysis, (i) July, (ii) August, (iii) September, (iv) October, (v) November.

The reasons for such a big difference could be due to the fact that the present region is covered mostly by forests and rainfall figures are much higher. As mentioned in the introduction, there are considerable spatial and temporal variabilities according to the climate of Ghana (Dickson & Benneh, 1995). These results could be improved if radio-sonde data for Ghana, were available to enable the actual temperature correction to be applied. As demonstrated by Carn & Lahuec (1990) the mapping procedure may be improve by incorporating a routine where it is checked if the area actually has been covered by cold possibly rain producing clouds. The land topography also varies much more compared to the Sahel (Eklundh, 1996, Kogan, 1990).

Conclusion

It has been shown that surface temperature-based rainfall estimation can be applied outside the Sahelian zone, even though the statistical relationships differ from what is obtained in the Sahelian studies. The estimates can be for periods longer than one month at least, to complement cold cloud methods on a short-term basis. These results could be improved if Radiosonde data were available for Ghana. Since clouds can be problematic in this area, albedo variance to delimit the clouds before carrying out the analysis can be used, which has been the case in this paper.

Acknowledgements

We are grateful to the Danish Meteorological Institute for the satellite images. Our thanks also go to the Ghana Meteorological Services Department for the rainfall data. This work was carried out at the Institute of Geography, Copenhagen, and in part at the Remote Sensing Research Unit of the Geography and Resource Development Department of the University of Ghana. We are grateful for the use of their facilities. Finally we wish to thank Charlotte Jespersen for reading and correcting the manuscript.

List of Acronyms

NOAA National Oceanic and Atmospheric Administration
AVHRR Advanced Very High Resolution Radiometer
AIVH (Name of METEOSAT product):

A: format = whole globe

I: Infra red

V: visible

H: high resolution (i.e. full data set no reduction).

References

- Brisson, A., P. Le Borgne & A. Marsouin (1990): Application of a satellite cloud classification scheme to a surface downward longwave flux calculations. *Proc. 8th METEOSAT Scientific User's Meeting*, 28 - 31 Aug., Norkoping, Sweden. EUM P08, ISBN 92-9110-002-1.
- Carn, M. & J.P. Lahuac (1990): The maximum radiative temperature: A major parameter in the estimation of rainfall over the Sahel using METEOSAT infrared images. *Proc. 8th METEOSAT Scientific User's Meeting*, 28 - 31 Aug., Norkoping, Sweden. EUM P08, ISBN 92-9110-002-1.
- CHIPS development team (1992): Chips satellite image processing system 3.0c, User's Guide. Institute of Geography, University of Copenhagen, Copenhagen, Denmark.
- Dickson, K.B. & G. Benneh (1995): A New Geography of Ghana, Longman Group Ltd., Essex, England.
- Eklundh, L. (1996): AVHRR NDVI for monitoring and mapping of vegetation and drought in East African environments. Ph.D. Thesis. Lund University.
- Guillot, G. (1995): Satellite et Précipitations: Contraintes techniques et physiques, analyse de quelques méthodes, problèmes de recherche et de validation. *Veille Climatique Stellaire* (France, Ministère de la Coopération) No.55, pp27-58.
- Gutman, G.G., A.M. Ignatov & S. Olson (1994): Towards better quality of AVHRR composite images over land: Reduction of cloud contamination. *Remote Sensing of Environment*. Vol.50, No.2, pp134-148.
- Holben, B.N. (1986): Characteristics of maximum-value composite images from temporal AVHRR data. *Int. J. Remote Sensing*, Vol7, No.11, pp1417 - 1434.
- Imbernon, J., J.P. Lagouarde, Y. Kerr & A. Begue (1990): Suivi agroclimatiques des cultures en zone Sahélienne. Report to EEC.
- Kakane, V.C.K. & J. Imbernon (1992): Estimation of Rainfall in the Senegal using the satellite NOAA-9/AVHRR. *Int. J. Remote Sensing*. Vol.13, No.11, pp2059-2068.
- Kogan, F.N. (1990): Remote sensing of weather impacts on vegetation in non-homogeneous areas. *Int. J. Remote Sensing*. Vol.11, No.8, pp1405-1419.
- Lagouarde J.-P., (1991): Use of NOAA AVHRR data combined with agro-meteorological model for evaporation mapping. *Int. J. Rem. Sens.* 12, 1853-1864.
- Meteosat Exploitation Project (1989): Meteosat-4 Calibration Report. Issue 1,2,3,4. European Space Operation Centre, Darmstadt, Germany.
- Milford, J.R. and Dugdale, G. (1990): Monitoring rainfall in real-time to control of migrant pests. *Phil. Trans. R. Soc. Lond. B* 328, 689-704
- Negre, T. (1987): Estimation et Suivi de la Pluviométrie au NEGAL par utilisation du Canal Infrarouge Thermique du Satellite METEOSAT. *Mémoire de fin d'études*, Institut National Agronomique. Paris-Grignon.
- Nicholson, S.E. (1994): Recent rainfall fluctuations in Africa and their relationship to past conditions over the continent. *The Holocene*, Vol.4, No.2, pp121- 131.
- Price, J.C. (1983). Estimation of Surface temperatures from

Conclusion

It has been shown that surface temperature-based rainfall estimation can be applied outside the Sahelian zone, even though the statistical relationships differ from what is obtained in the Sahelian studies. The estimates can be for periods longer than one month at least, to complement cold cloud methods on a short-term basis. These results could be improved if Radiosonde data were available for Ghana. Since clouds can be problematic in this area, albedo variance to delimit the clouds before carrying out the analysis can be used, which has been the case in this paper.

Acknowledgements

We are grateful to the Danish Meteorological Institute for the satellite images. Our thanks also go to the Ghana Meteorological Services Department for the rainfall data. This work was carried out at the Institute of Geography, Copenhagen, and in part at the Remote Sensing Research Unit of the Geography and Resource Development Department of the University of Ghana. We are grateful for the use of their facilities. Finally we wish to thank Charlotte Jespersen for reading and correcting the manuscript.

List of Acronyms

NOAA National Oceanic and Atmospheric Administration
AVHRR Advanced Very High Resolution Radiometer
AIVH (Name of METEOSAT product):

A: format = whole globe

I: Infra red

V: visible

H: high resolution (i.e. full data set no reduction).

References

- Brisson, A., P. Le Borgne & A. Marsouin (1990): Application of a satellite cloud classification scheme to a surface downward longwave flux calculations. *Proc. 8th METEOSAT Scientific User's Meeting*, 28 - 31 Aug., Norkoping, Sweden. EUM P08, ISBN 92-9110-002-1.
- Carn, M. & J.P. Lahuec (1990): The maximum radiative temperature: A major parameter in the estimation of rainfall over the Sahel using METEOSAT infrared images. *Proc. 8th METEOSAT Scientific User's Meeting*, 28 - 31 Aug., Norkoping, Sweden. EUM P08, ISBN 92-9110-002-1.
- CHIPS development team (1992): Chips satellite image processing system 3.0c, User's Guide. Institute of Geography, University of Copenhagen, Copenhagen, Denmark.
- Dickson, K.B. & G. Benneh (1995): A New Geography of Ghana, Longman Group Ltd., Essex, England.
- Eklundh, L. (1996): AVHRR NDVI for monitoring and mapping of vegetation and drought in East African environments. Ph.D. Thesis. Lund University.
- Guillot, G. (1995): Satellite et Précipitations: Contraintes techniques et physiques, analyse de quelques méthodes, problèmes de recherche et de validation. *Veille Climatique Stellaire* (France, Ministère de la Coopération) No.55, pp27-58.
- Gutman, G.G., A.M. Ignatov & S. Olson (1994): Towards better quality of AVHRR composite images over land: Reduction of cloud contamination. *Remote Sensing of Environment*. Vol.50, No.2, pp134-148.
- Holben, B.N. (1986): Characteristics of maximum-value composite images from temporal AVHRR data. *Int. J. Remote Sensing*, Vol7, No.11, pp1417 - 1434.
- Imbernon, J., J.P. Lagouarde, Y. Kerr & A. Begue (1990): Suivi agroclimatiques des cultures en zone Sahélienne. Report to EEC.
- Kakane, V.C.K. & J. Imbernon (1992): Estimation of Rainfall in the Senegal using the satellite NOAA-9/AVHRR. *Int. J. Remote Sensing*. Vol.13, No.11, pp2059-2068.
- Kogan, F.N. (1990): Remote sensing of weather impacts on vegetation in non-homogeneous areas. *Int. J. Remote Sensing*. Vol.11, No.8, pp1405-1419.
- Lagouarde J.-P., (1991): Use of NOAA AVHRR data combined with agro-meteorological model for evaporation mapping. *Int. J. Rem. Sens.* 12, 1853-1864.
- Meteosat Exploitation Project (1989): Meteosat-4 Calibration Report. Issue 1,2,3,4. European Space Operation Centre, Darmstadt, Germany.
- Milford, J.R. and Dugdale, G. (1990): Monitoring rainfall in realtaion to control of migrant pests. *Phil. Trans. R. Soc. Lond. B* 328, 689-704
- Negre, T. (1987): Estimation et Suivi de la Pluviométrie au NEGAL par utilisation du Canal Infrarouge Thermique du Satellite METEOSAT. *Mémoire de fin d'études*, Institut National Agronomique. Paris-Grignon.
- Nicholson, S.E. (1994): Recent rainfall fluctuations in Africa and their relationship to past conditions over the continent. *The Holocene*, Vol.4, No.2, pp121- 131.
- Price, J.C. (1983). Estimation of Surface temperatures from

- thermal infrared data. A simple formulation for the atmospheric effect. *Rem. Sens Env.* 13, pp 353-361.
- Rosema, A. (1982): Group Agromet Monitoring Project (GAMP) Final report, chp 7, Eur. Space Agency.
- Seguin, B., E. Assad, J.P. Freteaud, J. Imbernon, Y. Kerr, & J.P. Lagouarde (1989): Use of meteorological satellites for water balance monitoring in the Sahel region. *Int. J. Rem. Sens.* 10, 1011-1117.
- Søgaard, H (1988): Estimation of the surface energy balance in the Sahelian zone of Western Africa. *Geografisk Tidsskrift, Denmark*, vol 88 p 108-115.
- Søgaard, H (1989): A Comparison between satellite derived evapotranspiration and Normalized difference vegetation Index in the Sahelian Zone. *Proc of 22nd Int. symp. on Remote Sens. of Env.* Abidjan Vol I p 349-367
- Søgaard, H. (1990): Estimation of evapotranspiration in the Sahelian zone of Western Africa based on METEOSAT data. *Proc. 8th METEOSAT Scintific User's Meeting*, 28 - 31 Aug., Norkoping, Sweden. EUM P08, ISBN 92-9110-002-1.
- Stephens, G.L. (1994): *Remote Sensing of the Lower Atmosphere: An Introduction.* Oxford University Press, Oxford, U.K.

Conclusion

It has been shown that surface temperature-based rainfall estimation can be applied outside the Sahelian zone, even though the statistical relationships differ from what is obtained in the Sahelian studies. The estimates can be for periods longer than one month at least, to complement cold cloud methods on a short-term basis. These results could be improved if Radiosonde data were available for Ghana. Since clouds can be problematic in this area, albedo variance to delimit the clouds before carrying out the analysis can be used, which has been the case in this paper.

Acknowledgements

We are grateful to the Danish Meteorological Institute for the satellite images. Our thanks also go to the Ghana Meteorological Services Department for the rainfall data. This work was carried out at the Institute of Geography, Copenhagen, and in part at the Remote Sensing Research Unit of the Geography and Resource Development Department of the University of Ghana. We are grateful for the use of their facilities. Finally we wish to thank Charlotte Jespersen for reading and correcting the manuscript.

List of Acronyms

NOAA National Oceanic and Atmospheric Administration
AVHRR Advanced Very High Resolution Radiometer
AIVH (Name of METEOSAT product):

A: format = whole globe

I: Infra red

V: visible

H: high resolution (i.e. full data set no reduction).

References

- Brisson, A., P. Le Borgne & A. Marsouin (1990): Application of a satellite cloud classification scheme to a surface downward longwave flux calculations. *Proc. 8th METEOSAT Scientific User's Meeting*, 28 - 31 Aug., Norkoping, Sweden. EUM P08, ISBN 92-9110-002-1.
- Carn, M. & J.P. Lahuac (1990): The maximum radiative temperature: A major parameter in the estimation of rainfall over the Sahel using METEOSAT infrared images. *Proc. 8th METEOSAT Scientific User's Meeting*, 28 - 31 Aug., Norkoping, Sweden. EUM P08, ISBN 92-9110-002-1.
- CHIPS development team (1992): Chips satellite image processing system 3.0c, User's Guide. Institute of Geography, University of Copenhagen, Copenhagen, Denmark.
- Dickson, K.B. & G. Benneh (1995): A New Geography of Ghana, Longman Group Ltd., Essex, England.
- Eklundh, L. (1996): AVHRR NDVI for monitoring and mapping of vegetation and drought in East African environments. Ph.D. Thesis. Lund University.
- Guillot, G. (1995): Satellite et Précipitations: Contraintes techniques et physiques, analyse de quelques méthodes, problèmes de recherche et de validation. *Veille Climatique Stellaire* (France, Ministère de la Coopération) No.55, pp27-58.
- Gutman, G.G., A.M. Ignatov & S. Olson (1994): Towards better quality of AVHRR composite images over land: Reduction of cloud contamination. *Remote Sensing of Environment*. Vol.50, No.2, pp134-148.
- Holben, B.N. (1986): Characteristics of maximum-value composite images from temporal AVHRR data. *Int. J. Remote Sensing*, Vol7, No.11, pp1417 - 1434.
- Imbernon, J., J.P. Lagouarde, Y. Kerr & A. Begue (1990): Suivi agroclimatiques des cultures en zone Sahélienne. Report to EEC.
- Kakane, V.C.K. & J. Imbernon (1992): Estimation of Rainfall in the Senegal using the satellite NOAA-9/AVHRR. *Int. J. Remote Sensing*. Vol.13, No.11, pp2059-2068.
- Kogan, F.N. (1990): Remote sensing of weather impacts on vegetation in non-homogeneous areas. *Int. J. Remote Sensing*. Vol.11, No.8, pp1405-1419.
- Lagouarde J.-P., (1991): Use of NOAA AVHRR data combined with agro-meteorological model for evaporation mapping. *Int. J. Rem. Sens.* 12, 1853-1864.
- Meteosat Exploitation Project (1989): Meteosat-4 Calibration Report. Issue 1,2,3,4. European Space Operation Centre, Darmstadt, Germany.
- Milford, J.R. and Dugdale, G. (1990): Monitoring rainfall in real-time to control of migrant pests. *Phil. Trans. R. Soc. Lond. B* 328, 689-704
- Negre, T. (1987): Estimation et Suivi de la Pluviométrie au NEGAL par utilisation du Canal Infrarouge Thermique du Satellite METEOSAT. *Mémoire de fin d'études*, Institut National Agronomique. Paris-Grignon.
- Nicholson, S.E. (1994): Recent rainfall fluctuations in Africa and their relationship to past conditions over the continent. *The Holocene*, Vol.4, No.2, pp121- 131.
- Price, J.C. (1983). Estimation of Surface temperatures from